

**REACTION
ENGINEERING
INTERNATIONAL**

Committed Individuals Solving Challenging Problems

FIRESIDE MODELING IN CRACKING FURNACES

by

**Dr. David J. Brown, Stone & Webster Engineering Corporation
Dr. Marc A. Cremer/Prof. Philip J. Smith, Reaction Engineering Int'l
Dr. Richard T. Waibel, John Zink Company**

*Presented at the AIChE Ninth Annual Ethylene Producers Conference, March,
1997, Houston, TX, USA*

FIRESIDE MODELING IN CRACKING FURNACES

1.0 INTRODUCTION

At the 6th Ethylene Producers' Conference in Atlanta, Georgia a paper was presented which described the first stage of development of the use of modeling of the fireside of ethylene furnaces (Brown, Smith and Adams, 1994). Since that time several detailed simulations have been undertaken for a range of different types of furnaces. This paper describes some of the more interesting results of that work.

2.0 BACKGROUND

Through an alliance between Stone & Webster Engineering Corporation (SWEC) and Reaction Engineering International (REI), detailed computer simulation of conditions within the radiant section of cracking furnaces are being performed. These simulations use a computational fluid dynamic (CFD)-based turbulent reacting flow code which couples together the effects of turbulent fluid mechanics, homogeneous gas-phase and heterogeneous particle phase combustion chemistry, and conductive, convective, and radiative heat transfer within the radiant firebox. Two-way coupling between the fire-side and tube-side conditions exists so that heat transfer into the process tubes is dependent on both the tube and fire-side conditions.

Using a tool which provides full coupling of all relevant physical processes within the radiant firebox allows the designer to determine sensitivities to design changes without relying on simplified empirical models that are often extrapolated beyond the conditions for which their validity has been proved. This, indeed, is precisely what is described in the following examples.

3.0 OVERVIEW OF MODEL

The computational tools used by Reaction Engineering International (REI) are based on software developed over the last two decades by Prof. Philip J. Smith, Vice President of REI, and his students and colleagues at the University of Utah and REI. The current software simulates reacting and nonreacting flow of gases and particles, including gaseous diffusion flames, pulverized-coal flames, liquid sprays, coal slurries, isothermal and reacting two-phase flows, injected sorbents, and other oxidation/reduction systems. These software tools have been applied to a wide variety of industrial systems encompassing utility boilers, pyrolysis furnaces, gas turbine combustors, rotary kilns, waste incinerators, smelting cyclones and others. These applications have been used for basic design, problem solving, pollution control, etc. using many different fuels including natural gas, coal, and waste.

The model used specifically for the simulation of process heaters provides full coupling between the "fire-side" and "process-side" computations. Heat transfer between the process coils and the hot radiant fire-box depends on the process fluid temperature, the overall heat transfer coefficient from the process fluid to the hot coil surface, the fire-side temperature distribution, and the local

flow field. The heat transferred to the process fluid affects the local chemical composition and temperature which is then fed back to the fire-side computations. Further details concerning how this is accomplished in the model are discussed in the following two sections.

3.1 Fire-Side Modeling

3.1.1 Gas Phase Combustion

The computational approach involves numerical discretization of the partial differential equation set which describes the physics of the system. Typically 10^5 - 10^6 discrete computational nodes are needed to resolve the most relevant features of a three-dimensional combustion process. Around 60 variables (representing, e.g., gas velocity, temperature, concentration of various chemical species) are tracked at each node. Accurate simulation of the combustion processes requires accurate modeling of the dominant or controlling physical mechanisms in the process. Simulation of process temperatures in a process heater requires modeling of the flow patterns, reaction chemistry, gas and wall temperatures, heat transfer in the furnace (fireside), and heat transfer and temperature change in the process fluid (process side). In the computer model used here, coupled equations of chemical reaction, turbulent fluid flow, and convective and radiative heat transfer are solved to give a realistic and detailed model of the processes taking place within the fired zone.

Turbulence is modeled using traditional methods of moment closure including Prandtl's mixing length model, the two-equation k-e model (Launder and Spalding, 1972) and the nonlinear k-e

model (Speziale, 1987). In all simulations discussed in this report, the nonlinear k-e model was used due to its more accurate prediction of normal Reynolds stress effects, allowing the prediction of secondary flows as occur in non-circular ducts.

Within the model, the rate at which the combustion reactions occur is assumed to be limited by the rate of mixing between the fuel and the oxidizer. That is, the rate of chemical reactions is assumed to be fast compared to the rate of mixing (i.e. full chemical equilibrium is assumed), which is a reasonable assumption for the chemical reactions governing heat release. The thermochemical state at each spatial position is a function of the degree of mixing (parametrized by the mixture fraction, f), the mass fraction of particle off-gas (h), and the enthalpy (parametrized by the degree of heat loss, HL). The effect of turbulence on mean chemical composition is incorporated by assuming that the mixture fraction at each spatial position is described by a “clipped-gaussian” probability density function (PDF) having spatially varying mean, and variance. Mean species concentrations are obtained by convolution over this assumed PDF.

Since the rates governing the formation and destruction of NO_x are of the same order of magnitude as those governing mixing, the assumption that chemical reaction is fast compared to mixing is inaccurate for these species. To account for the rate of formation of these species in the model, additional equations governing the formation of thermal, prompt, and fuel NO_x are solved in a “post process” analysis. These equations can be de-coupled from the equations governing the turbulent flow field since the formation of these trace species has little effect on the velocity field. Thus, the converged velocity field is used in the equations governing NO_x .

Since radiation is typically the most significant mode of heat transfer to the process coils in a process furnace, it is critical that the radiation field be accurately represented. Accurately simulating radiative transfer to specific regions in a system requires a model which can account for both absorbing-emitting radiation processes and complex system geometries, including arbitrary structures such as process coils. Additionally, it is desirable that any radiative model selected be computationally efficient in terms of execution time and storage to allow coupling with other routines in a comprehensive combustion model. REI's process heater model utilizes the discrete-ordinates method which has been shown to be a good choice for modeling radiation in combustion systems, both in terms of computational efficiency and accuracy. This method retains the directional dependency of the radiation intensity in a way that other flux models are unable to achieve, yet provides for a finite-difference or finite-volume solution that is more computationally efficient than zone methods and more deterministic than Monte Carlo methods. The development of the discrete-ordinates method and its application to a number of complex geometries (e.g., Adams, 1993; Adams and Smith, 1993) have been presented in the literature and serve to validate the use of this method in accurately modeling radiative heat transfer in process heaters (Adams, 1993; Adams & Smith, 1993; Adams & Smith, 1995).

3.1.2 Particle Phase Combustion

Along with the capability of modeling gas phase combustion and turbulent transport, the model is also equipped to handle condensed phase turbulent transport, dispersion, and reaction. This

capability makes possible the simulation of practical combustion processes which use solid particles, liquid droplets, or slurries as fuels in turbulent environments. In the context of modeling cracking furnaces, this capability makes possible the simulation of oil or coal fired furnaces or coke particle burnout within the radiant firebox during decoking operations. Predictions of simulations of this latter application are discussed in section 4.2.

The turbulent transport of particles is solved for in a Lagrangian reference frame by modeling the time evolution of a probability density function (PDF) for the particle position. The value of this time evolving PDF, at any location, represents the probability of finding particles of the corresponding type and starting position, with that residence time, at that location in the flow field. This probability is used to obtain the expected number density of particles with the corresponding properties in each computational volume. The contribution to mass, momentum, and energy by these particles in each Eulerian computational cell is added dynamically while tracking the particle PDF to provide source terms which are coupled into the Eulerian gas phase transport equations. The mean particle position and its variance are expressed as ordinary differential equations, with the aerodynamic drag force and weight providing the main driving force for mean particle position change and the fluctuating component of velocity determining the variance about this value. Further details describing the methodology used for modeling turbulent particle transport are available elsewhere (Baxter, 1989; Jain, 1996, Smoot, 1985).

Within the model, the three mechanisms for mass loss of each particle are vaporization, devolatilization, and heterogeneous reaction. The overall rate of reaction of each type of particle

is found by solution of governing continuity equations for each of these processes. The kinetic parameters that are used are based on independent experimental observations and kinetic parameters deduced from these observations. In the context of coke particles in a process heater, the particle is considered to consist of four components: liquid, raw coke, char, and ash. Reaction rates for these components are computed based on local gas properties which affect heat transfer and mass transfer to the particle. On the other hand, mass evolved from each particle due to vaporization, devolatilization, or char oxidation is locally incorporated into the Eulerian gas phase computations. In particular, this approach leads to a comprehensive strategy for representing coke particle transport and burnout within the radiant firebox of a full-scale process heater. Further specific details concerning particle phase reactions are available elsewhere (Baxter, 1989; Smoot, 1985).

3.2 Process-Side Modeling

To accurately predict heat transfer to the process side fluid, the fire-side conditions must be coupled with the process side. The energy absorbed into the process coils acts to heat up the fluid and provide energy for the endothermic cracking reactions. This process temperature affects the convective heat transfer on the inside tube wall as well as the outside tube metal temperature and finally, the net heat flux to the coil. Thus, the process and fire-side conditions are tightly coupled and must be modeled as such.

The approach used for providing this coupling in the simulations discussed in this report was as follows. Using a detailed simulation of the kinetics and heat transfer inside the tubes coupled with a relatively simple model of external heat transfer to the tubes, SWEC obtained tabulated data of process temperature and heat transfer coefficient versus cumulative absorbed duty for each firing condition. Since the overall heat transfer coefficient is dependent on tube diameter, this correlation was also tabulated as a function of tube diameter. This relationship was then used within the comprehensive model to provide the link between absorbed duty, heat transfer coefficient, and process temperature. In other words, given the absorbed duty as predicted by the comprehensive model, this relationship provided the appropriate process temperature and heat transfer coefficient at each grid location along the process coil.

In principle, the process-side chemistry model should be fully coupled with the fire-side combustion and heat transfer model since variation in the external heat transfer to the process coils, as predicted by the comprehensive model, could potentially affect the relationship between absorbed duty and process temperature. However, calculations performed by SWEC indicate that this level of coupling is not necessary and that the simplified model of external heat transfer, based on a given heat flux profile, is sufficiently accurate to identify the relationship between absorbed duty and process temperature. This is not to say that the external heat flux profile is not important with respect to its effect on process temperature, but that the distribution of heat transfer to the tubes has a relatively small effect on the correlation between cumulative absorbed duty and process temperature.

3.3 Model Inputs

In addition to the necessary geometrical information, simulation of conditions within the radiant section of a process heater requires the specification of several model inputs. Among these are the following:

- Tube model
- Tube thermal resistance
- Refractory wall thermal resistance
- Tube and refractory wall emissivity
- Fuel composition, temperature, and mass flow rate
- Oxidizer composition, temperature, and mass flow rate

The manner in which conditions on the process-side are coupled with those on the fire-side is what is here termed the "tube model". The model used in the present simulations involves using a tabulated correlation between cumulative absorbed energy, process temperature, and the process-side heat transfer coefficient. The internal heat transfer coefficient as well as the tube wall thickness and thermal conductivity are used to determine the overall tube thermal resistance, R_t , between the fire-side tube wall and the process side fluid. This wall resistance represents the total resistance to heat transfer by series conduction through the tube wall, the coke layer formed on the inside wall, and by forced convection from the inside tube wall to the process fluid.

Generally, the fire-side tube metal temperature (TMT) is not known, a priori, and must be determined from an energy balance at the surface. The balance may be written as

$$q''_{rad} + q''_{conv} = q''_{cond} = \frac{T_s - T_b}{R_f} \quad \text{Eq. 1}$$

where q''_{rad} , q''_{conv} , and q''_{cond} represent net radiative, convective, and conductive fluxes, respectively, at the surface. Assuming that the flameside convection coefficient (computed by the model), incident radiative flux, surface emissivity, backside temperature (T_b , process temperature), and the conductive thermal resistance (R_f) are known, the surface temperature, T_s , can be found.

In a similar manner, thermal boundary conditions for the furnace refractory walls must be specified. As a percentage of the furnace fired duty, heat loss through the furnace walls typically ranges from 1-3%. Although small, this heat loss is not negligible and the spatial dependency of these losses within the furnace should be modeled. The thermal resistance, R_f , between the fireside refractory wall and the outside ambient air is specified taking into account the conduction through the refractory material and convection from the outside wall to ambient conditions. As R_f approaches infinity, heat loss through the furnace walls approaches zero. Using Eq. 1, along with assumed data for refractory wall emissivity, the furnace wall temperature, T_s , can be computed.

Finally, thermo-chemical data for all inlets must be specified. Usually this requires specification of temperature, composition, and mass flow rate of a fuel stream and an air stream. When two-phase

flows are modeled, as in the simulation of decoking operations inside the firebox of a process heater, the composition, temperature, and mass flow rate of the particulate phase must also be specified.

4.0 SIMULATIONS

Computer simulations were recently carried out for two full scale ethylene cracking furnaces. The primary objectives of these simulations were to:

- Confirm required fuel firing rate to achieve the specified heat transfer to the coils
- Predict the coil to coil variation in process fluid outlet temperature
- Quantify the amount of flow pass balancing required to minimize coil outlet temperature (COT) deviations
- Predict the overall flow field, coke particle trajectories, and burnout during decoking back to the firebox

4.1 Furnace 1 - Normal Firebox Operation

The first radiant firebox modeled is approximately 35 ft. high, 60 ft. long, and 10.0 ft. wide. There are twelve simple serpentine M coils aligned vertically in a plane passing through the center of the

furnace as shown in Fig. 1. Each coil consists of three vertical inlet passes or tubes and three vertical outlet passes. The coil is swaged, so that the three final passes are larger in diameter than the three inlet passes. Due to the symmetry of the radiant firebox, only one-half of it was modeled by placing a symmetry plane through the center as shown in Fig. 1

The firebox is completely floor-fired using 24 burners distributed in two rows placed adjacent to the furnace walls. The burners are spaced so that the centerline of each burner corresponded with the centerline of the opposing process coil as shown in Fig. 1. The burners are nonpremixed staged gas burners with internal flue gas recirculation (John Zink designation PSFFR) as shown in Fig. 2.

4.1.1 Baseline Simulations

For this furnace, baseline simulations were performed for three firing conditions:

- Normal firing conditions
- Maximum firing conditions
- Design firing conditions

Model inputs which were varied for these three cases included the overall fuel firing rate, the feedstock, both quantity and composition, (this affected the tube model), and the fuel composition.

The correlations between process side temperature and cumulative absorbed duty, based on SWEC analyses, that were used for these simulations are shown in Fig. 3.

The predicted COTs for the three modeled conditions are shown in Fig. 4, and the corresponding predicted refractory wall temperatures are shown in Fig. 5. All three simulations indicated the presence of a significant cool end wall effect at a constant firing rate and constant flow to each coil. Fig. 4 shows that a variation in COTs of approximately +/- 10 °F can be expected with the third and fourth coils from the end wall yielding the highest COT and the first coil, the lowest. This variation can be seen to be related to the distribution of refractory wall temperature and the local gas temperature. For all three modeled conditions, Fig. 5 shows that as a function of furnace length, the refractory wall temperature mirrors the temperature distribution witnessed in the COTs. The wall temperature increases from a minimum near the end wall and peaks in the vicinity of the third burner from the end wall. This behavior is also apparent in the distribution of gas temperature as seen in Fig. 6 for the normal firing condition. The cooler end wall temperature is explicitly shown in Fig. 7 in which its temperature is compared with that of the front and back furnace wall. Fig. 7 shows that the end wall temperature is significantly cooler than the adjacent walls. The overall temperature of the front wall is also predicted to be noticeably cooler than the back wall (where the back wall is defined to be the wall having the flue gas take off running along the top).

It is believed that the temperature distribution within the furnace can be explained in part by the velocity field within the firebox. The three-dimensional flow field predicted for this furnace is

relatively complex. The hot gas adjacent to the furnace walls flows upward from the floor burners. Some of this gas proceeds out the flue gas exit, but a portion of it turns toward the center of the furnace and flows downward adjacent to the tubes and is later re-entrained by the burners near the floor. The asymmetrical placement of the flue gas outlet results in the asymmetrical flow on either side of the row of coils. One effect of this asymmetry is a difference in temperature between the front wall of the furnace (the wall opposite the flue gas outlet) and the back wall, as can be seen in Fig. 7. This difference in temperature is most dramatic in the upper half of the furnace. This effect can be seen in Fig. 8 which shows front and back wall temperature versus furnace height for the normal firing condition. The suspected reason for the temperature difference is that hot gas from the floor burners travels up the entire length of the back wall prior to turning and exiting out the flue gas outlet along this wall. On the other hand, gas from the floor burners along the front wall travels only part of the distance up the wall prior to separating from the wall to turn and exit out the flue gas outlet along the opposite side. This separation causes a region of recirculating gas along the top of the front wall which is relatively cool, and thereby cools the upper half of the front wall.

In a similar manner, the noticeably cooler temperature of the furnace end wall may be explained. Fig. 7 shows refractory temperature versus wall length for the end wall, front wall, and back wall. Clearly, the end wall of the furnace is significantly cooler than the other two walls. The predicted velocity field shows the existence of relatively cool recirculating gas toward the top of the end wall. This gas has a similar cooling effect on the end wall as was discussed before for the front wall. The effect of this relatively cool end wall is reduced radiative heat transfer to the end coils. The

effects of this are witnessed as a reduction in process fluid temperature, coil outlet temperature, etc.

4.1.2 Flow Pass Balancing

An important control objective is to minimize the deviation in COTs from coil to coil so that, as far as possible, each coil operates at the same conversion and cokes at the same rate. In the Atlanta paper (Brown, Smith and Adams, 1994) the efficacy of zone firing was evaluated. For this furnace flow pass balancing is used which one convection pass for each symmetrical, adjacent pair of back to back coils.

Simulations for all three of the firing conditions modeled in the baseline study predicted a significant effect of the end walls on heat transfer to the coils. The predictions indicated a dominant profile in the COTs in which coils 1 and 2 have the lowest COT and coils 3 and 4 the highest. Pass varying the mass flow rates through the process coils, increasing the mass flow rate if the COT is too high or decreasing it if the COT is too low. The relative amount of modulation is governed by:

$$q_2 = q_1(m_2 / m_1) \quad \text{Eq. 2}$$

where the process fluid temperature T corresponds to the cumulative absorbed duty q_1 (q_2) and process mass flow rate m_1 (m_2). This expression reflects conservation of energy in that when the

process mass flow rate is increased, ($m_2 / m_1 > 1$) a larger amount of energy, q_2 , must be absorbed to bring the process temperature up to the same level, T.

Simulations to test the feasibility of using flow rate modulation had to abide by the constraints of the expected control system for the overall fuel firing rate and the process mass flow rates. The overall fuel firing rate is governed by the average of the 12 coil outlet temperatures, and the mass flow rates to adjacent coil pairs is varied depending on the pair-wise averages of the COTs. The objective of this system is to obtain:

$$\frac{1}{2} \sum_{n=i}^{i+1} COT(n) = \frac{1}{12} \sum_{n=1}^{12} COT(n) \quad \text{Eq. 3}$$

for $i=1,3,5,7,9$, and 11.

To demonstrate that the statement of Eq. 3 is achievable using the control system described above, a simulation was performed using model inputs for the normal firing condition. The level of flow rate modulation predicted prior to the simulation was based on the energy transferred to each pair of coils in the baseline simulation of normal firing conditions. Based on this information and application of Eq. 2, a prediction of the percentage decrease or increase in the mass flow rate was made and input to the model. The total process flow rate was not changed. Flow rate modulation to adjacent coil pairs did not exceed 1.3% of the baseline mass flow rates. The mass flow rate to

coils 1 and 2 was decreased, that to coils 3 and 4 was increased, and that to coils 5 and 6 was decreased.

4.2 Furnace 2 - Decoking Operations

Thermal cracking of hydrocarbons is always accompanied by coke formation. During normal operation, coke slowly deposits on the inside walls of the process coils, leading to reduced heat transfer to the process fluid and increased pressure drop, and eventually plugged coils in the most extreme case. Depending on the feedstock, the severity of cracking, and the type of furnace, the run length can vary from days to months.

To burn off the coke from the tube walls, the furnace has to be periodically shut down to perform decoking operations. Typically, a combination of high temperature air and steam is passed through the process coils to both blast the coke off the walls and partially oxidize it inside the coils. The unburnt coke and gaseous products can then either be collected for disposal or re-routed back into the firebox for subsequent burnout. Simulations discussed in this section relate to modeling conditions inside the firebox during the latter type of decoke operation.

Issues of concern in burning out the residual coke inside the firebox that were addressed in these simulations included:

- Effect of the decoke effluent on the overall flow and heat transfer inside the firebox

- Trajectories of the coke particles as they relate to impingement on tube and refractory walls
- The efficiency of coke particle burnout

Although process side conditions were coupled with fireside conditions as previously discussed, particular issues related to coke burnout inside the process tubes were not addressed in these simulations. The effluent exiting the decoke nozzles was assumed to be at a fixed mass flow rate, temperature, gas composition, particle mass fraction, and particle size distribution based on SWEC analysis and empirical data. Process temperature inside the process coils as well as the tube metal temperature was computed as before using the approach outlined in section 3.2.

Decoking conditions were simulated in the firebox shown in Fig. 11. This furnace which is approximately 35 ft. high, 100 ft. long, and 10 ft. wide and has 96 U-coils grouped into 8 coil modules (or 12 coils each) aligned along the center of the furnace. The furnace is fired by 32 PSFFR burners positioned uniformly along the opposing furnace walls as shown in Fig. 12. The eight decoke nozzles were placed in the floor and positioned between the first and second burners and the fifth and sixth burners from the end wall as also shown in Fig. 12. Due to the symmetry of this furnace only one-half was modeled and a symmetry boundary condition was used at the furnace centerline.

Notable observations that were made in the simulation of decoking were the following:

- The high momentum flow from the decoke nozzles governs the overall flow pattern in the furnace
- Changing the nozzle geometry (circular inlet vs. rectangular inlet) significantly alters the overall fluid mechanics in the furnace
- Circular inlets appear to entrain flue gases more uniformly leading to a more uniform temperature distribution in the furnace.
- Coke particles smaller than 250 mm burnout quite efficiently while being convected by the recirculating gases in the furnace.
- Coke particles larger than 250 mm impinge on the radiant roof and fall back to the floor where they burnout.

5.0 ON-GOING WORK

Designing a burner which simultaneously meets the requirements of stability, flexibility, good heat transfer distribution and the regulatory emission limits is somewhat empirical. Often the needs conflict with each other, which eventually leads to a compromise configuration which can only be proven by extensive testing in a test furnace. Even after the test of a single burner, the direct correlation between single burner and multiple burner performance is somewhat uncertain. Currently REI, SWEC and John Zink Company are working in close collaboration to develop and prove the capability of the software to assist in the development of new and improved burner analysis.

6.0 CONCLUSIONS

The three dimensional simulation of turbulent combustion and heat transfer within the radiant section of a cracking furnace provides for a detailed examination of the effects of design and operating changes on process side conditions. Since the fire-side conditions are coupled with the process side conditions, nonlinear effects associated with changing firing rates, coil and furnace geometry, firing distribution, feedstock, and process flow rates can be examined in a rigorous manner. In particular, it was shown how these simulations can be used to determine the feasibility of obtaining uniform coil outlet temperatures by independently modulating the process mass flow rates.

The ability to model turbulent transport and reaction of particles also makes it possible to investigate furnace conditions during decoking operations. These investigations can be used to guide the design and placement of nozzles to efficiently burn coke within the radiant firebox without significantly altering the overall heat transfer to the coils or damaging the refractory and coil walls by particle impingement.

The modeling techniques are currently being extended into the area of burner design.

REFERENCES

Adams, B. R., "Computational evaluation of mechanisms affecting radiation in gas and coal fired industrial furnaces," Ph.D. Dissertation, Department of Mechanical Engineering, University of Utah, (1993).

Adams, B. R., and Smith, P. J., "Three-Dimensional discrete-ordinates modeling of radiative transfer in a geometrically complex furnace," *Combust. Sci. and Tech.*, **88**, 293 (1993).

Adams, B. R., and Smith, P. J., "Modeling effects of soot and turbulence-radiation coupling on radiative transfer in turbulent gaseous combustion," *Combust. Sci. and Tech.*, **109**, 121 (1995).

Baxter, L. L., "Turbulent transport of particles," Ph.D. Dissertation, Department of Chemical Engineering, Brigham Young University, Provo, UT (1989).

Brown, D. J., Smith, P. J. and Adams, B. R., "Cracking Furnace Fireside Modeling Advances," Paper presented at the AIChE Spring National Meeting, EPC Conference (1994).

Jain, S., "Three-Dimensional simulation of turbulent particle dispersion applications," Ph.D. Dissertation, Department of Chemical and Fuels Engineering, University of Utah (1996).

Smoot, L. D. and Smith, P. J., *Coal Combustion and Gasification*, Plenum Press, New York (1985).

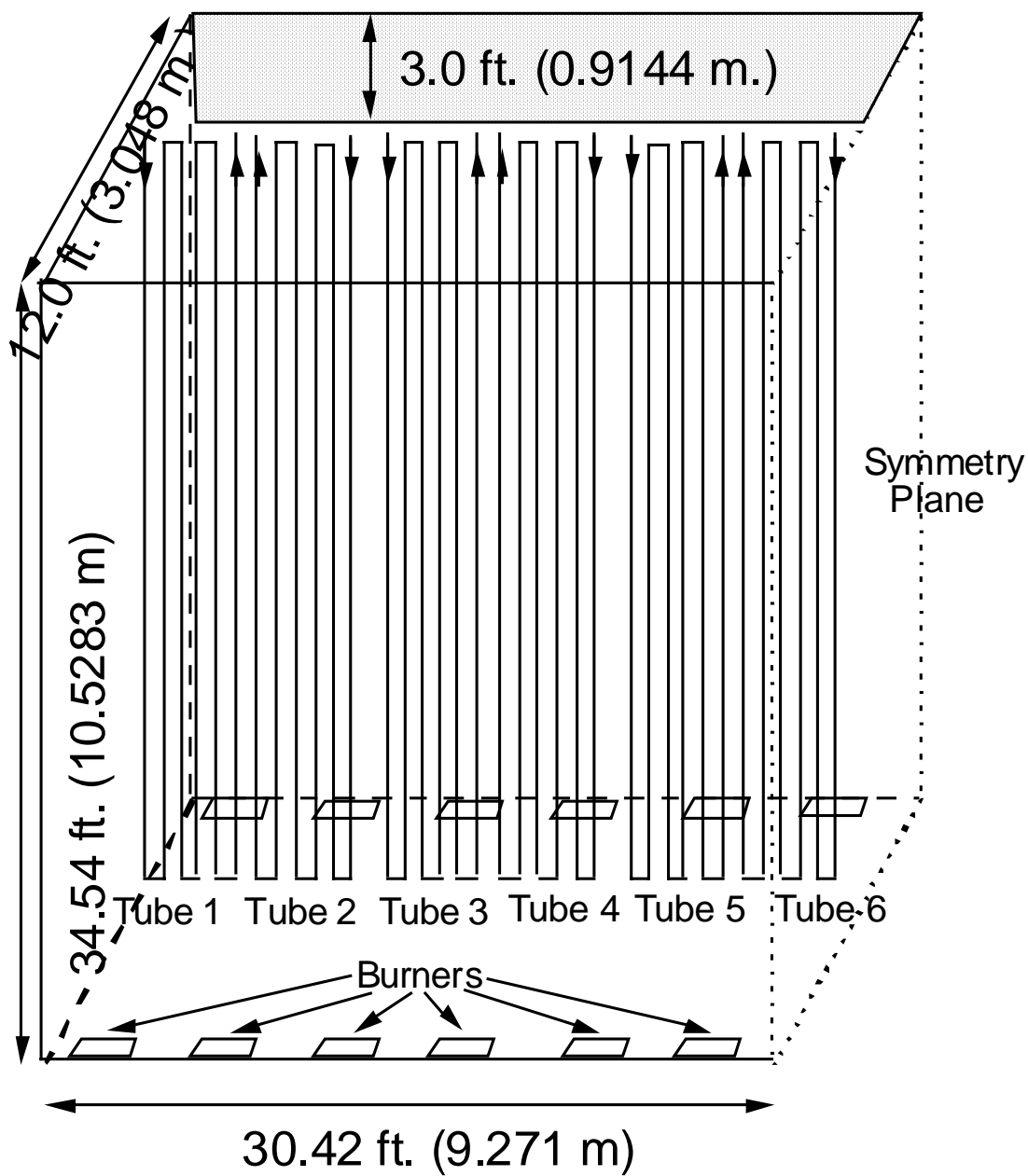


Figure 1: Schematic of modeled 12 serpentine coil ethylene cracking furnace.

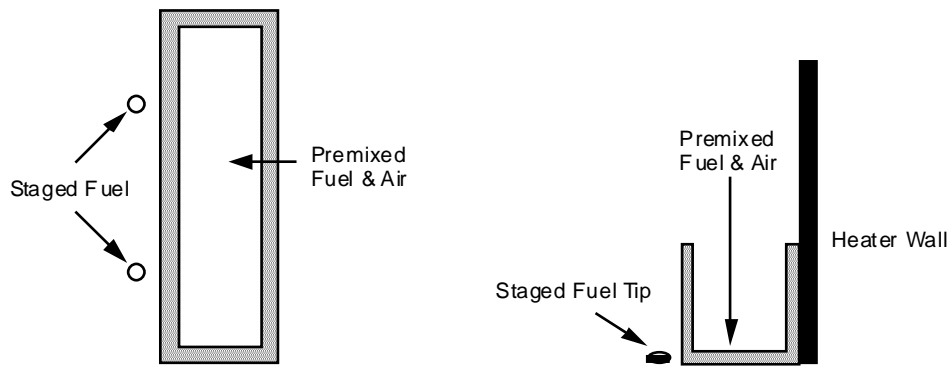


Figure 2: Model description of staged floor burner.

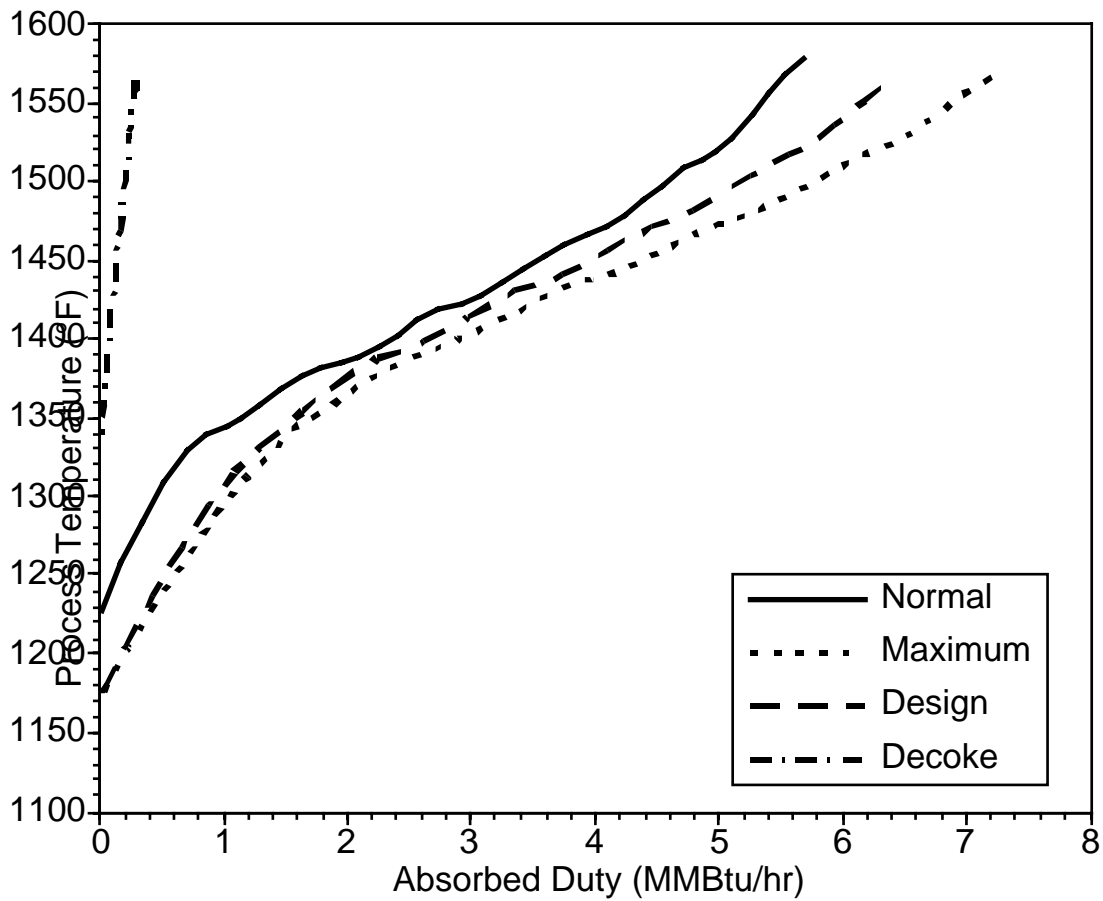


Figure 3: Correlations between absorbed heat and process temperature for each modeled condition.

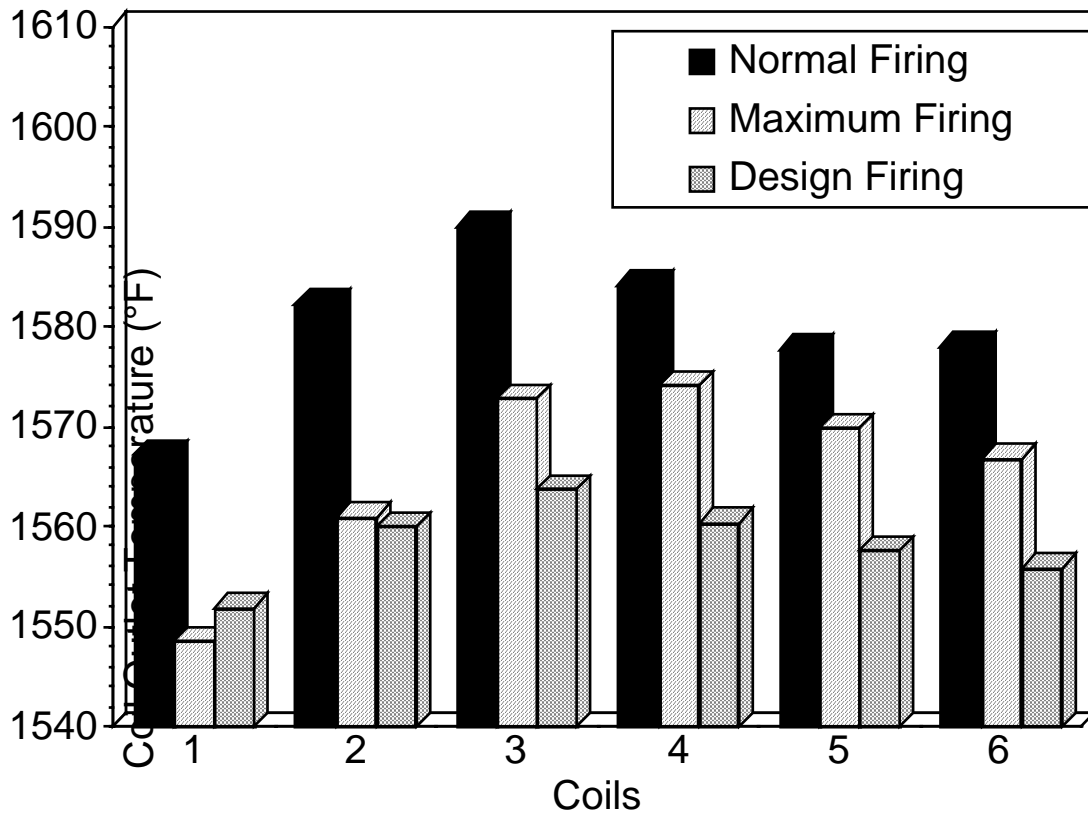


Figure 4: Comparison of predicted coil outlet temperatures for three firing conditions.

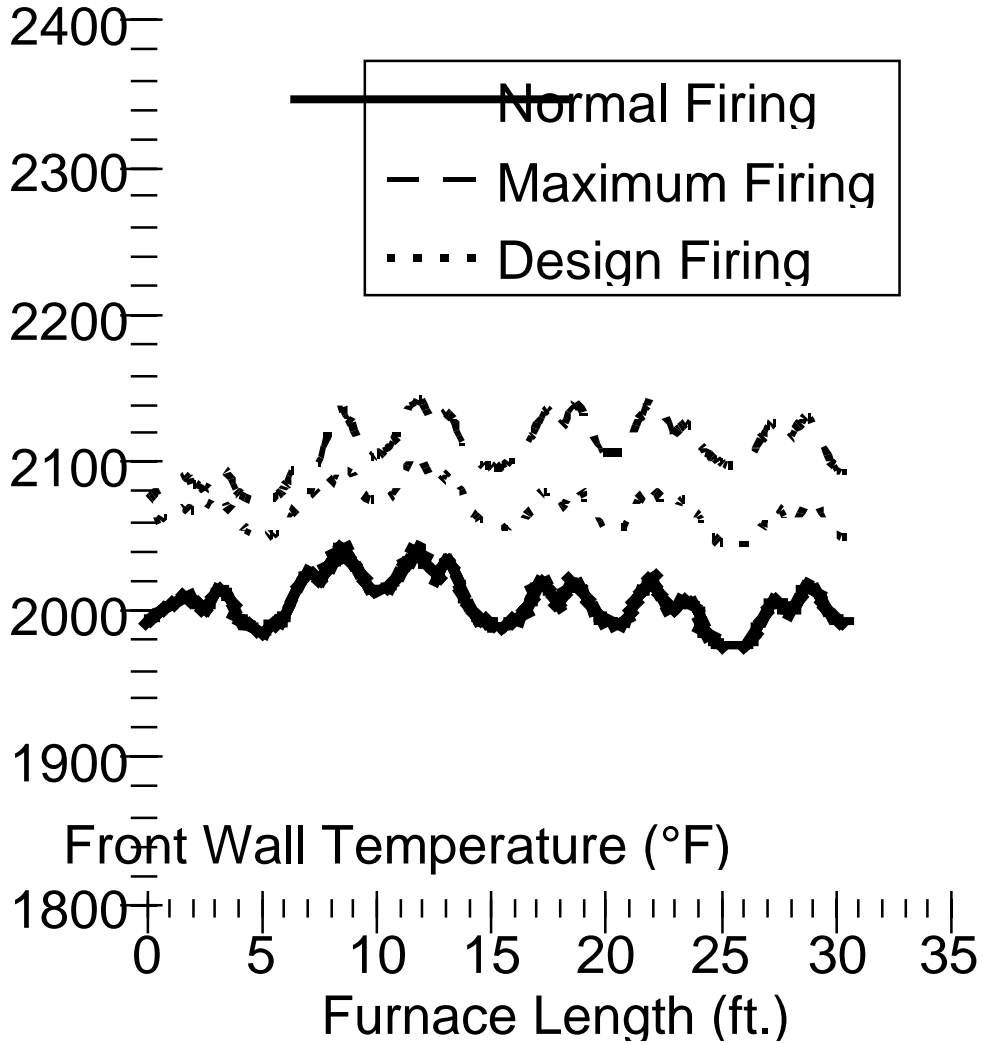


Figure 5: Comparison of predicted wall refractory temperature versus furnace length for three firing conditions.

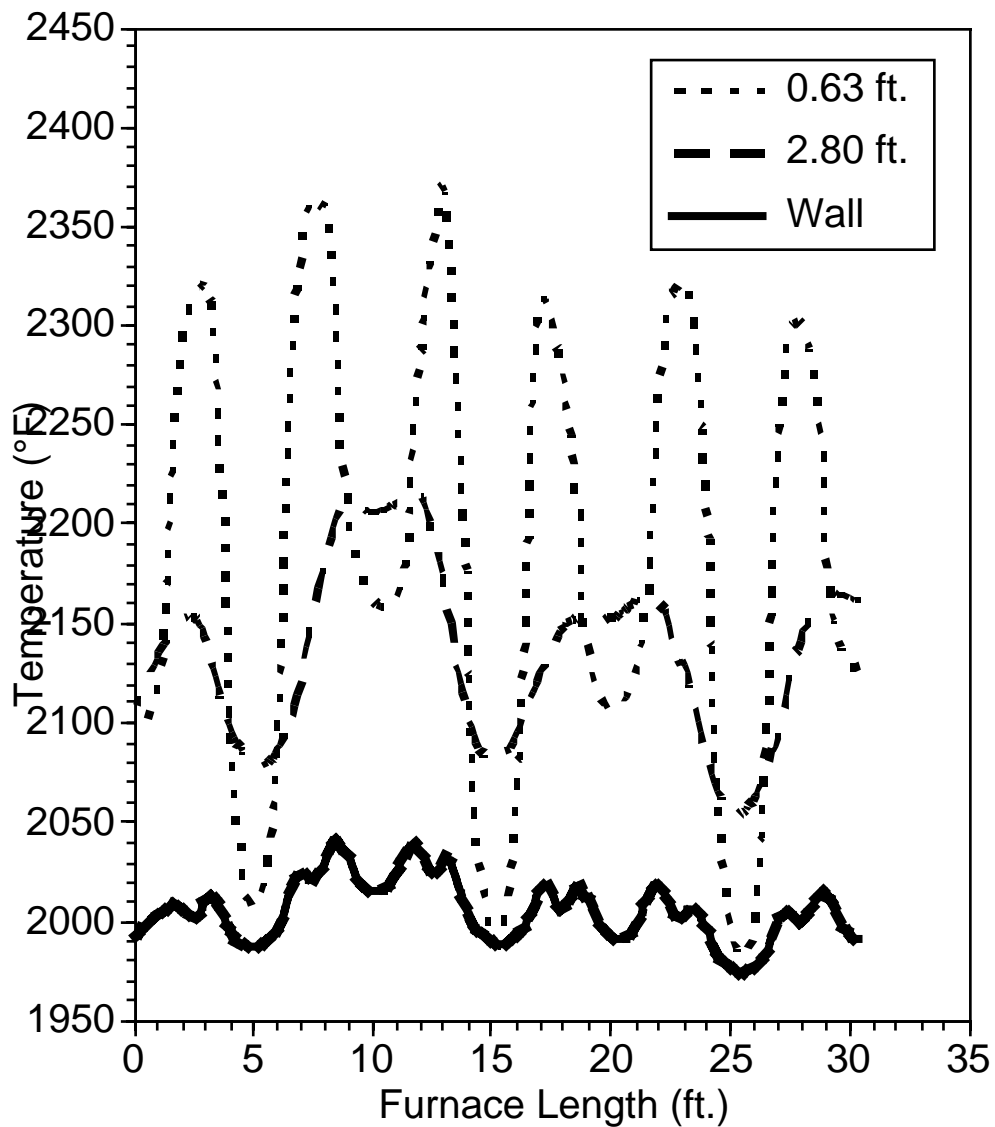


Figure 6: Predicted furnace front wall and gas temperature versus furnace length during normal firing conditions. Temperature at each point is an average over the furnace height. Gas temperature is plotted at 2 locations measured from the furnace wall.

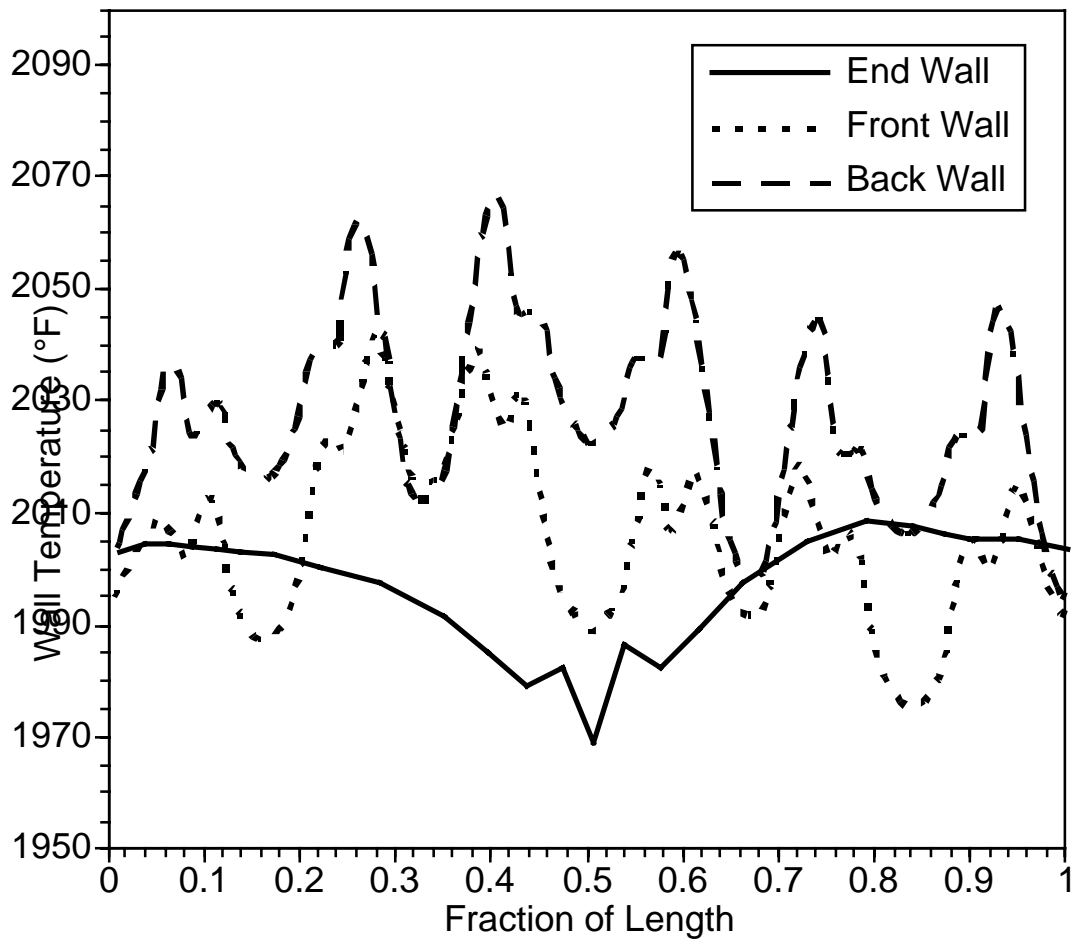


Figure 7: Comparison of refractory wall temperature versus wall length. Wall length is represented as a fraction of total length (actually half the side wall length) so that all three plots can be shown on the same scale. The wall temperatures are averaged over the height of the wall. The end wall temperature is significantly cooler than the front and back wall temperatures.

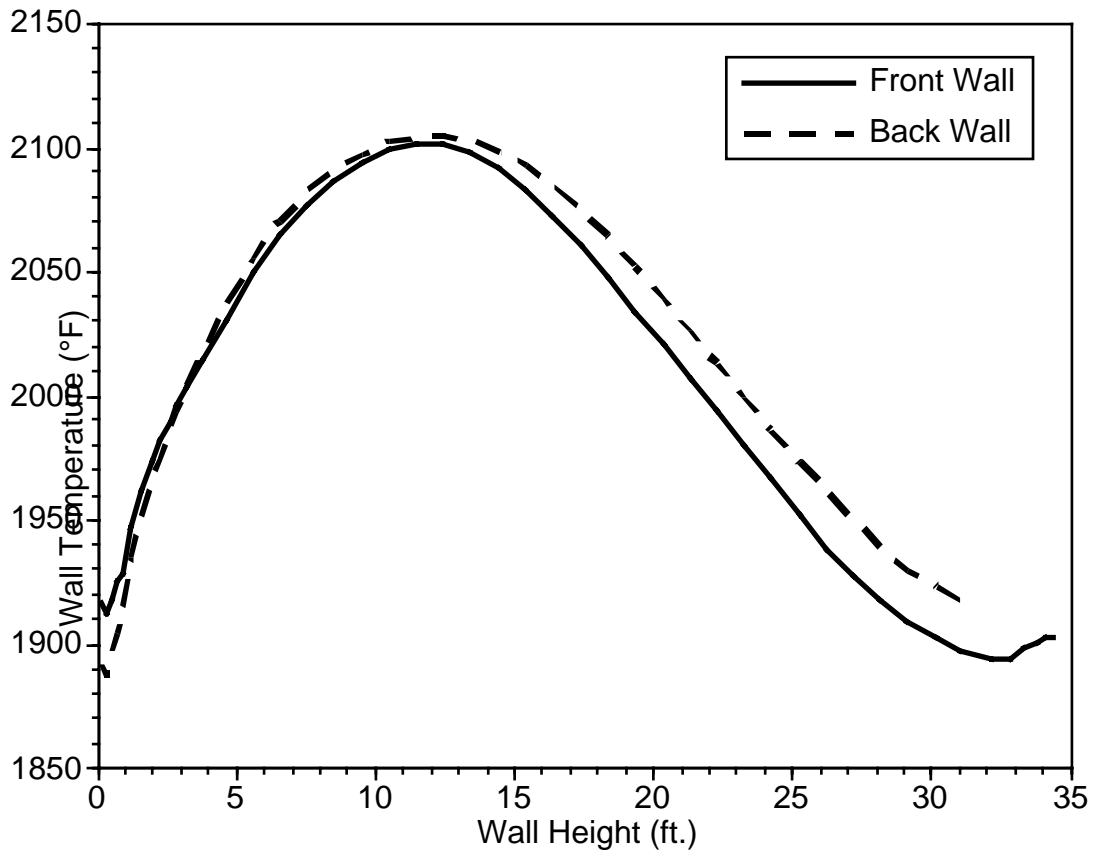


Figure 8: Comparison of front and back refractory wall temperature. The front wall, opposite the flue gas outlet, is cooler than the back wall temperature near the top of the furnace.

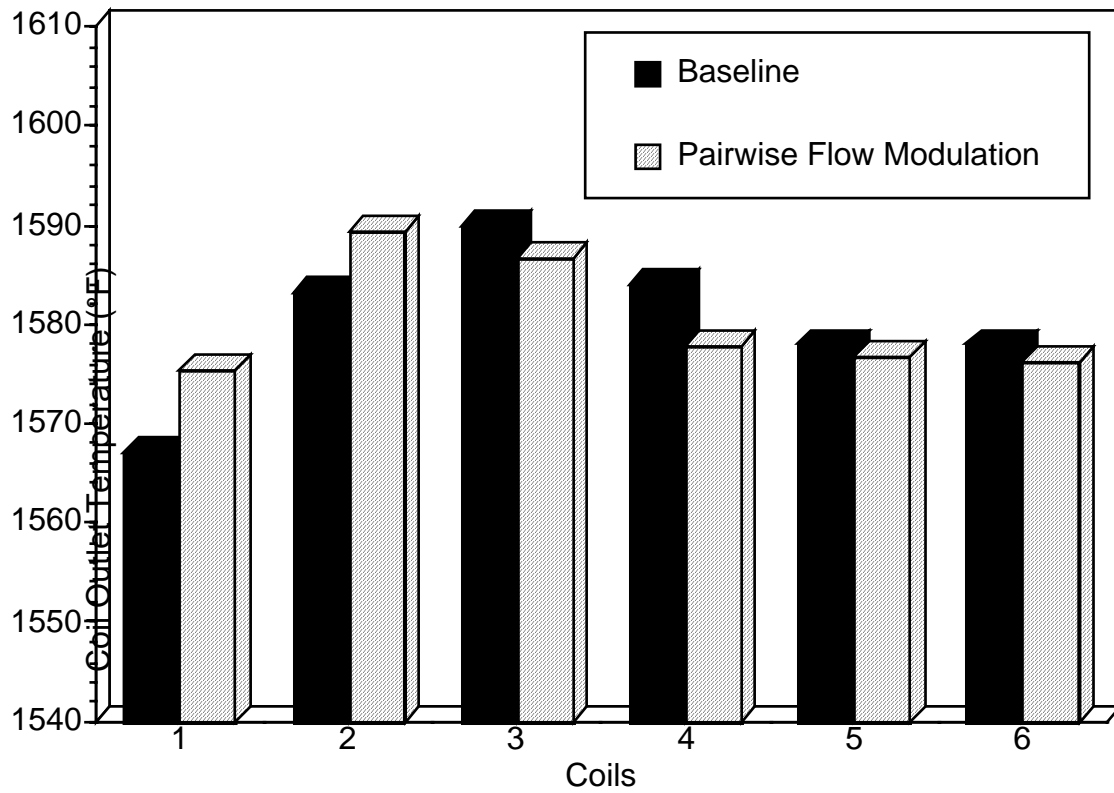
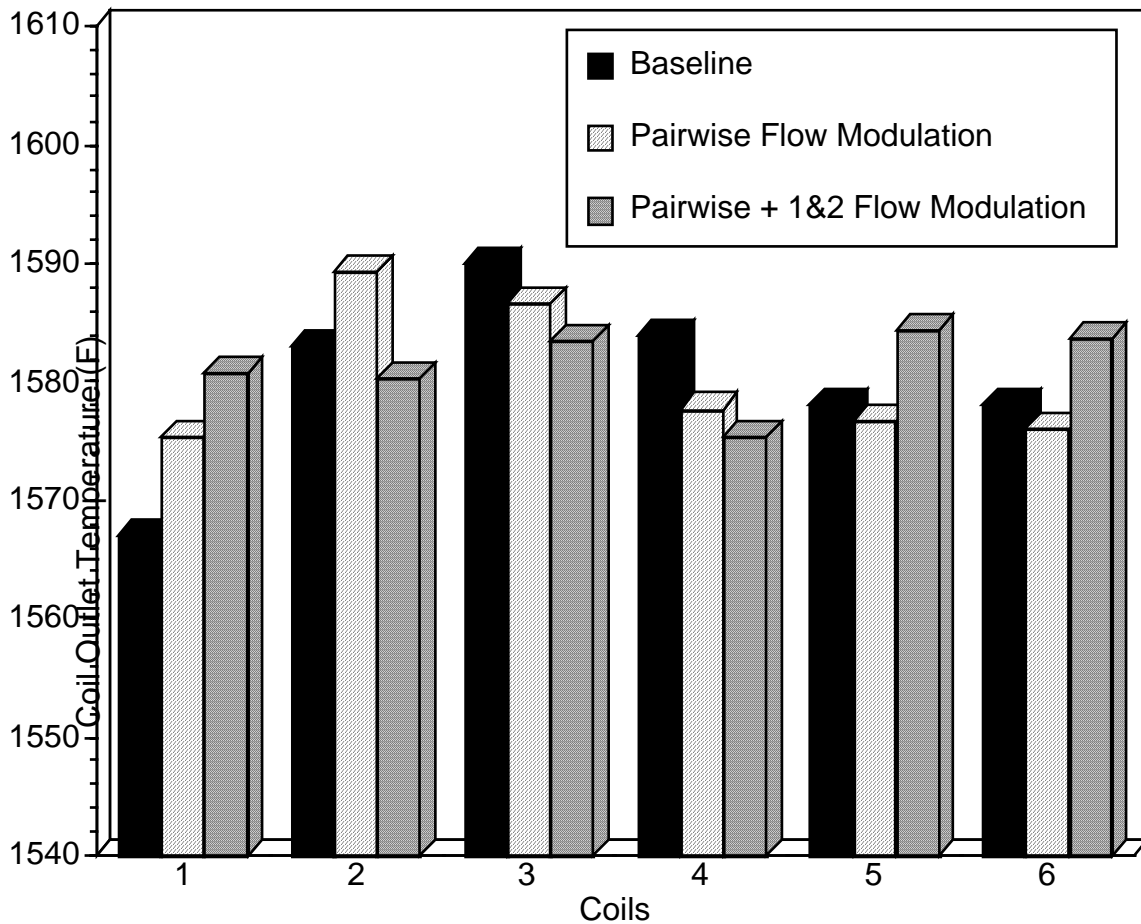


Figure 9: Comparison of coil outlet temperature for normal firing conditions with and without pair-wise flow rate modulation.



Figure

re 10: Comparison of predicted coil outlet temperature with and without process flow rate modulation. In the baseline case, the coil flow rates are uniform. Pair-wise flow rate modulation denotes changes to flow rates to adjacent coil pairs. Pair-wise +1&2 flow modulation denotes pair-wise flow rate modulation along with independent flow modulation for coils 1 and 2. In all cases the total mass flow rate is unchanged.

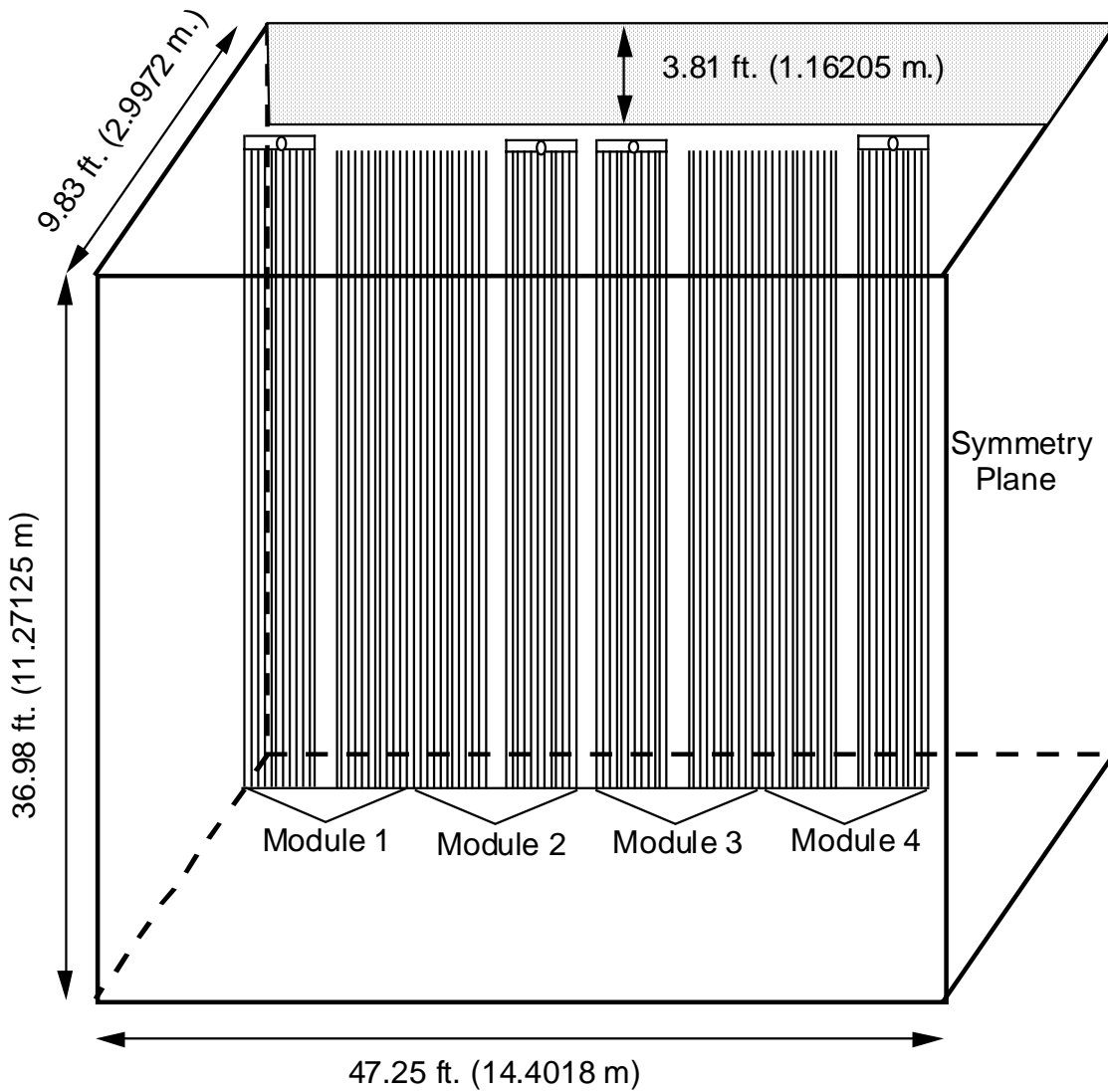


Figure 11: Simulated "U coil" furnace.

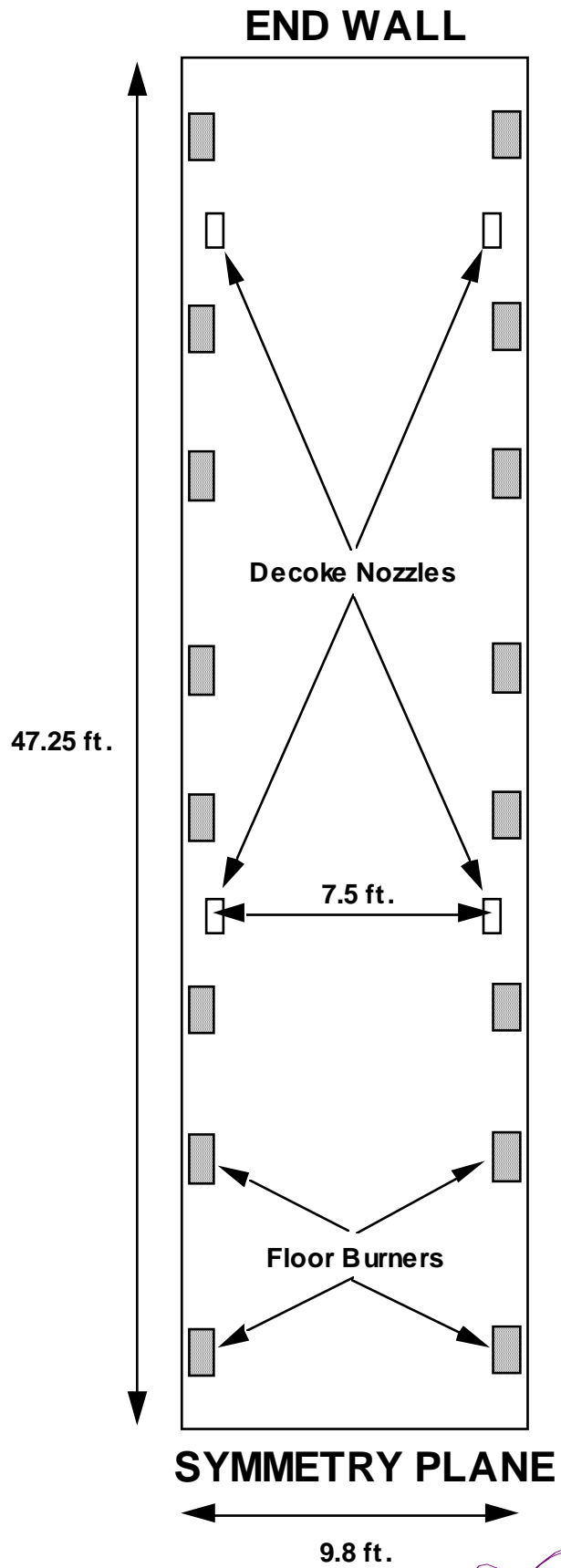


Fig. 10.2.1.1. Schematic diagram of the end wall.